IMPACTO CIENTÍFICO EDITORA

ANALYTICAL AND NUMERICAL STUDY OF COMPOSITE FLAT ROOFS CONTAINING PLASTERBOARD AND AÇAÍ PIT RESIDUE

ESTUDO ANALÍTICO E NUMÉRICO DE TETOS PLANOS COMPOSTOS CONTENDO PLACA DE GESSO E RESÍDUO DO CAROÇO DO AÇAÍ

ESTUDIO ANALÍTICO Y NUMÉRICO DE TECHOS PLANOS COMPUESTOS QUE CONTIENEN PLACAS DE YESO Y RESIDUOS DEL PEPITA DEL AÇAÍ

https://doi.org/10.56238/edimpacto2025.089-005

Ubiraci Silva Nascimento[1], Marcio da Silva Tavares[2], Edvan Moreira[3], Fernando Lima de Oliveira[4], José de Ribamar Pestana Filho[5], Valter Valder Reis Beckman[6], Lucas Santos de Oliveira[7], Izak Oliveira Sousa da Silva[8], Isabelle Cristina dos Reis de Andrade Batista[9], João Pedro Silva Lima[10], Gleuberth Ruan Pontes Coelho[11], Pedro Victor Braga Dias[12]

ABSTRACT

In this project, we used concepts of thermal conductivity and heat transfer applied to flat ceilings, exploring the fact that thermal conductivity varies from material to material, thus providing an opening in the range of studies in the area of mathematical and numerical analysis of this variation. To this end, a MATLAB code was used, applying the explicit MDF - finite difference method in the explicit model, starting from the discretization of the thermal diffusion equation, where the simulations were performed based on data obtained from the thermophysical properties of materials found in the literature, as well as data obtained experimentally, where the thermal conductivities and specific mass of gypsum boards with different additions of açaí pulp biomass were used. The analyses focused on evaluating the

[1] Dr in Mechanical Engineering. Universidade Estadual do Maranhão (UEMA). Maranhão, Brazil.
Orcid:0000-0002-4069-601X
[2] Dr. in Physics. Universidade Estadual do Maranhão (UEMA). Maranhão, Brazil.
Orcid:0000-0002-3832-3492
[3] Post-Doctorate in Physics. Universidade Estadual do Maranhão (UEMA). Maranhão, Brazil.
Orcid:0000-0002-5610-2757
[4] Dr. in Mechanical Engineering. Universidade Estadual do Maranhão (UEMA). Maranhão, Brazil.
Orcid:0009-0001-2876-2766
[5] Master of Science in Education. Universidade Estadual do Maranhão (UEMA). Maranhão, Brazil.
E-mail: ssjpestana@gmail.com
[6] Physics Specialist. Universidade Estadual do Maranhão (UEMA). Maranhão, Brazil.
Orcid:0009-0003-9300-1693
[7] Doctorate in Mechanical Engineering. Universidade Estadual de Campinas (UNICAMP). São Paulo, Brazil.
Orcid:0000-0001-7478-1477
[8] Graduating in Civil Engineering. Universidade Estadual do Maranhão (UEMA). Maranhão, Brazil.
E-mail: izakoliver.eng.br@outlook.com
[9] Undergraduate student in Civil Engineering. Universidade Estadual do Maranhão (UEMA). Maranhão, Brazil.
E-mail: isabelle.20220058337@aluno.uema.br
[10] Graduating in Civil Engineering. Universidade Estadual do Maranhão (UEMA). Maranhão, Brazil.
E-mail: joãopedroengciviluema@gmail.com
[11] Graduating in Civil Engineering. Universidade Estadual do Maranhão (UEMA). Maranhão, Brazil.
E-mail: Gleuberth.20220058159@aluno.uema.br
[12] Graduating in Civil Engineering. Universidade Estadual do Maranhão (UEMA). Maranhão, Brazil.
E-mail: pdiaxxvi@gmail.com

effects of varying the percentage of biomass added to the gypsum boards and the thickness of the ceiling, as well as analyzing and comparing the efficiency of flat ceilings made with different types of materials. We intend for the results of this study to contribute to another construction alternative, with an emphasis on the thermal aspect of environments.

Keywords: Numerical Analysis. Açaí. Biomass. Ceilings. Sustainability.

RESUMO

Usamos neste projeto, conceitos de condutividade térmica e transferência de calor aplicados em tetos planos, explorando o fato de que a condutividade térmica varia de material para material, proporcionando assim, uma abertura no leque de estudos na área de análise matemática e numérica dessa variação. Para tanto, foi usado um código em MATLAB, aplicando o MDF- método de diferenças finitas no modelo explícito, partindo da discretização da equação de difusão térmica de calor, onde as simulações foram realizadas a partir de dados obtidos das propriedades termo físicas de materiais existentes em literatura, assim como dos dados obtidos experimentalmente, onde foram usados as condutividades térmicas e massa específica das placas de gesso com diferentes adições de biomassa do caroço do Açaí. As análises foram concentradas para avaliar os efeitos na variação do percentual da biomassa adicionada às placas de gesso, espessura do teto, além de analisar e comparar a eficiência de tetos planos feitos com diferentes tipos de materiais. Pretendemos com os resultados desse estudo, está contribuindo com mais uma alternativa de construção, dando-se ênfase ao aspecto térmico de ambientes.

Palavras-chave: Análise Numérica. Açaí. Biomassa. Tetos. Sustentabilidade.

RESUMEN

En este proyecto utilizamos conceptos de conductividad térmica y transferencia de calor aplicados a techos planos, explorando el hecho de que la conductividad térmica varía de un material a otro, lo que abre un abanico de estudios en el área del análisis matemático y numérico de esta variación. Para ello, se utilizó un código en MATLAB, aplicando el MDF , método de diferencias finitas en el modelo explícito, a partir de la discretización de la ecuación de difusión térmica del calor, donde las simulaciones se realizaron a partir de datos obtenidos de las propiedades termofísicas de materiales existentes en la literatura, así como de datos obtenidos experimentalmente, donde se utilizaron las conductividades térmicas y la masa específica de las placas de yeso con diferentes adiciones de biomasa del carozo del açaí. Los análisis se centraron en evaluar los efectos de la variación del porcentaje de biomasa añadida a las placas de yeso y el espesor del techo, además de analizar y comparar la eficiencia de los techos planos fabricados con diferentes tipos de materiales. Con los resultados de este estudio, pretendemos contribuir con otra alternativa de construcción, haciendo hincapié en el aspecto térmico de los ambientes.

Palabras clave: Análisis Numérico. Açaí. Biomasa. Techos. Sostenibilidad.

1 INTRODUCTION

This work focuses on the use of the addition of açaí seed residue to plaster molded in plate shapes, as a construction alternative, as a filling of flat roofs, in order to evaluate its performance in a numerical way, emphasizing the thermal aspect. It was structured in such a way that initially bibliographic reviews of the state of the art were carried out by consulting several current articles that address the subject, then we will present a numerical model containing governing equations, initial conditions, boundary conditions and method of resolution (PATANKAR, 1980).

The search for an effective, resistant and cheap thermal insulating material for buildings is constantly being the focus of more recent scientific research (FAQ, 2015).

Ceilings also have the ability to prevent blocking the sun's rays and thus not letting the environment heat up. It is possible to do some special treatments to make it more efficient in blocking the sun's rays (ÇENGEL 2012).

The production and use of materials with better thermal efficiencies becomes an alternative for investment in low-cost buildings, thus benefiting from access to a housing unit for low-income populations.

Lima (2005) developed a research on composite material for use in civil construction, using plaster mortar and vegetable fiber, with the objective of obtaining a new material that can be used as a coating or sealing elements, adding to this property that leads to low thermal conductivity. The tests carried out indicated that the thermal properties of the Vegetable Fiber provided a gain of 27.14% in thermal insulation by reducing the thermal conductivity of the compound.

Barbosa *et al*. (2019), in a study to characterize açaí particles aiming at their potential use in civil construction, evaluated açaí residues (*Euterpe oleracea and Euterpe precatoria*) characterizing them physically, chemically, thermally and morphologically. Density tests were carried out by pycnometry, verification of moisture content, and lignin, cellulose and extractive contents, according to the normative parameters of TAPPI 204, 211 and 222. The result of the average density of the particles is 1.49 g/cm3, with moisture content ranging from 2 to 6%. Regarding the chemical composition, it was observed higher levels of lignin and extractives, and a reduction of cellulose in relation to other vegetable fibers. Scanning Electron Microscopy (SEM) showed the presence of only the endocarp of the açaí seed in the 8 and 14 Tyler particles, and a greater predominance of fibers in the 48, 100 and 200 Tyler particles. The knowledge of the physicochemical characteristics of açaí waste particles

is necessary to support composite processing steps using these materials. In addition, the use of a waste such as açaí seeds enhances the reduction of environmental impacts, providing, especially for civil construction, the possibility of producing new, more ecological materials, generating sustainability indicators in buildings in the Amazon region.

The relevance of this project is very great and comprehensive, considering that it deals with a current environmental problem and associates a new technology to solve thermal comfort problems in a sustainable way, saving energy and reducing environmental impacts.

2 METHODOLOGY

The analytical study with the Numerical Simulation can be carried out at home, without the need to use UEMA's facilities, a fact that was motivated by the suspension of face-to-face activities, due to the restrictions imposed by the COVID-19 pandemic, the same happened online, including simultaneously carrying out the activities of the other experimental project. These steps can go hand in hand without compromising your results. For the numerical simulation solution, a program was developed to be run in MATLAB.

There are different numerical methods that can be used for the problem at hand. The finite difference method is the simplest, but it can be inaccurate when there are multiple bodies in contact. Finite element and finite volume methods are better suited to studying multiple bodies in contact, but are more computationally complex. For this and for the sake of practicality, the code was discretized and implemented by the mathematical model MDF – Finite Difference Method.

The modeling started from the equation of one-dimensional thermal diffusion in transient regime for heat conduction along a wall without internal heat generation. This equation is a Parabolic Partial Differential Equation and, for the case under study, it is of the nonlinear type since the boundary conditions are functions of the independent variable time, since it is assumed that the solar radiation incident on the surface of the external wall and the daily environmental temperature vary throughout the hours of the day (DUFFIE & BECKMAN, 2013). Due to these characteristics, it is necessary to use a numerical method to obtain the solution of the equation. Thus, it was decided to use MDF with Explicit Scheme due to its simplicity, vast available literature and satisfactorily representing unidirectional heat transfer phenomena.

The use of the method boils down to working the phenomenon in a discrete domain of points, whose equations are linear and simpler to solve than if they were worked in the

continuous domain. Thus, an important step of the method is the discretization step of the heat diffusion equation to the points inside the body of the ceiling and at its internal and external borders. And, taking into account that our ceiling is formed by more than one material arranged in layers, we have to admit each layer as a body with two borders, which makes the process much more complex and laborious.

Flat roofs in hot countries are usually subject to high solar radiation and transmit a large part of this incident solar energy to the internal environment, causing thermal discomfort to the occupants. Boards composed of gypsum and residue from the Açaí seed can be used for insulation of flat roofs in order to reduce the incident radiation transmitted. Since these slabs can be placed in parallel with the concrete layer, because the slabs do not mix with the concrete, there is no change in the mechanical characteristics of the same. A typical flat roof in Brazil is typically composed of a 20 mm thick outer layer of waterproof cement mortar, 150 mm thick concrete slab, and 20 mm thick inner layer of finishing mortar (NASCIMENTO, 2020).

The Figure below illustrates the composite ceiling, which was designed for the assembly of the algorithm, initially containing 05 (five) layers and 11 (eleven) points of interest to be considered for the elaboration of mathematical modeling and subsequent simulations.

Figure 1

Composition of the Composite Ceiling with points of interest

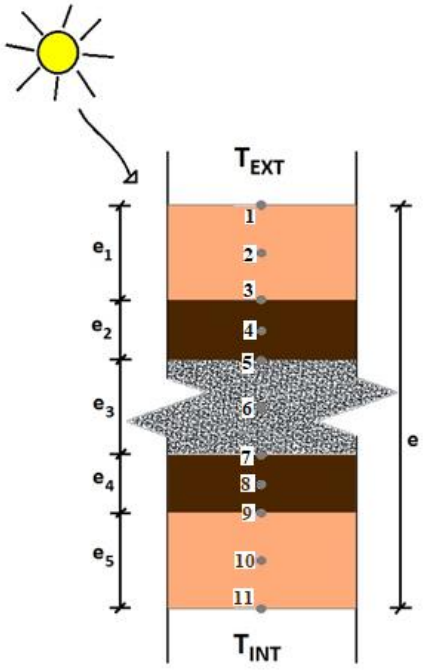

Source: Authors (2022).

It is convenient to note that, although an algorithm has been used for five layers, there is the possibility of working with layers of numbers smaller than five up to a single one. For our study, all layers were considered to be homogeneous, considering that:

- Each constituent layer of the elements of our ceiling is homogeneous and isotropic;
- The thermal properties of the materials that make them up do not vary with temperature;
- There are no heat sources inside the elements;
- There are no considerations or infiltration of moisture in the elements;
- Boundary conditions are symmetrical.

3 RESULTS AND DISCUSSIONS

3.1 DISCRETIZATION OF THE THERMAL DIFFUSION EQUATION

To begin the discretization, it is important to highlight that our thermal roof is composed of a flat surface that receives solar radiation, convection on the external and internal surface, conduction through the ceiling, conduction between the internal borders of the ceilings and pure conduction between the plaster ceiling. We consider the uniform initial temperature, constant physical properties of building materials, convection heat transfer coefficient on the internal and external faces, humidity-free ceiling, and constant internal air temperature.

To obtain the governing equation of the problem, we will take as a basis the formulation of finite differences (PATANKAR, 1980).

By the definition of derivative:

$$\frac{\partial f}{\partial x} = \frac{f(x+\Delta x) - f(x)}{\Delta x} \qquad (1)$$

If we make the first derivative by the truncated Taylor series (x+ Δx around x) and also the first derivative truncated in n=1. And rearranging the equation obtained, we will reach an equation similar to the definition of the derivative (1) below:

$$\frac{\partial T(x)}{\partial x} = \frac{T(x+\Delta x) - T(x)}{\Delta x} \qquad (2)$$

Making the second derivative for the point m:

$$\frac{\partial^2 T(x)}{\partial x^2}_m = \frac{\frac{\partial T(x)}{\Delta x}_{m+1/2} - \frac{\partial T(x)}{\Delta x}_{m-1/2}}{\Delta x} \quad (3)$$

$$\frac{\partial T(x)}{\Delta x}_{m+1/2} = \frac{T_m - T_{m-1}}{\Delta x} \; ; \; \frac{\partial T(x)}{\Delta x}_{m-1/2} = \frac{T_{m+1} - T_m}{\Delta x} \quad (4)$$

We will use the substitution of equation (4) in equation (3), we will get:

$$\frac{\partial^2 T(x)}{\partial x^2}_m = \frac{\frac{T_m - T_{m-1}}{\Delta x} - \frac{T_{m+1} - T_m}{\Delta x}}{\Delta x} \quad (5)$$

Achieving then:

$$\frac{\partial^2 T(x)}{\partial x^2} = \frac{T_{m-1} - 2T_m + T_{m+1}}{\Delta x^2} \quad (6)$$

In the case of transient heat conduction, the governing equation is derived from the first law of thermodynamics and the Fourier equation for diffusion heat flux.

$$\frac{\partial^2 T}{\partial x^2} + \frac{\partial^2 T}{\partial y^2} + \frac{\partial^2 T}{\partial z^2} + \frac{e_{ger}}{k} = \frac{1}{\alpha}\frac{\partial T}{\partial t} \quad (7)$$

For the case of heat conduction in a one-dimensional transient regime in a flat wall and without heat generation, we have the following equation:

$$\frac{\partial^2 T}{\partial x^2} = \frac{1}{\alpha}\frac{\partial T}{\partial t} \quad (8)$$

3.1.1 Discretization within each layer

For a discretization of the inner knots at the points (2; 4; 6; 8 and 10) of Figure 1, making the appropriate energy balances for the explicit method, is as follows, as shown in Figure (2) and Equation (9):

Figure 2

Dots inside the mesh

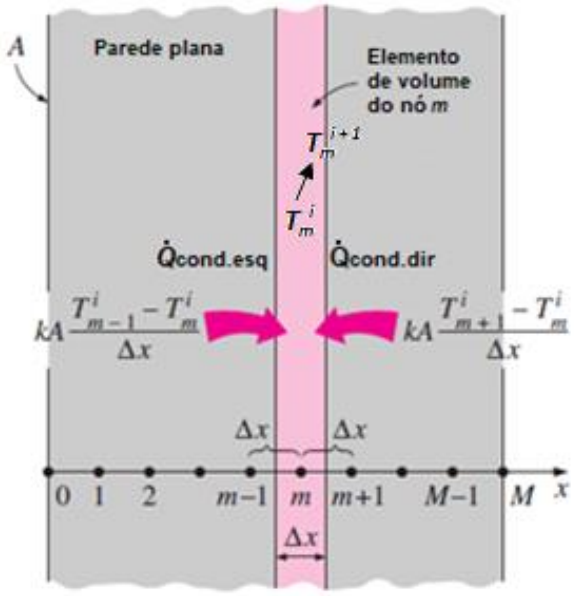

Source: Çengel, adapted.

By performing the energy balance or substituting equation (6), we obtain the equation:

$$kA\frac{T_{m-1}-T_m}{\Delta x}+kA\frac{T_{m+1}-T_m}{\Delta x}=\rho A\Delta x C_p\frac{T_m^{i+1}-T_m^i}{\Delta t} \quad (9)$$

Multiplying by Δx/(kA), we get:

$$T_{m-1}-2.T_m+T_{m+1}=\frac{\rho.\Delta x^2}{k}c_p\frac{T_m^{i+1}-T_m^i}{\Delta t} \quad (10)$$

Para: $(\alpha=\frac{k}{\rho.c_p})$, fica: $$T_{m-1}-2.T_m+T_{m+1}=\frac{\Delta x^2}{\alpha\Delta t}(T_m^{i+1}-T_m^i) \quad (11)$$

Sendo $(\tau=\frac{\alpha\Delta t}{\Delta x^2})$, teremos: $$T_{m-1}-2.T_m+T_{m+1}=\frac{T_m^{i+1}-T_m^i}{\tau} \quad (12)$$

Explaining the term of interest and reorganizing the previous equation, we have:

$$T_m^{i+1}=(T_{m-1}-2T_m+T_{m+1})\tau+T_m^i \quad (13)$$

3.1.2 Discretization between different layers

In Figure 1, we have the points (3; 5; 7 and 9) for the problem of heat conduction between the walls of different materials, where we have to assume for this discontinuity, the change of the material from one plate to another and that the knot of the mesh is at the exact point between the two bodies, as shown in Figure 3 below.

Figure 3

Knot between the two plates

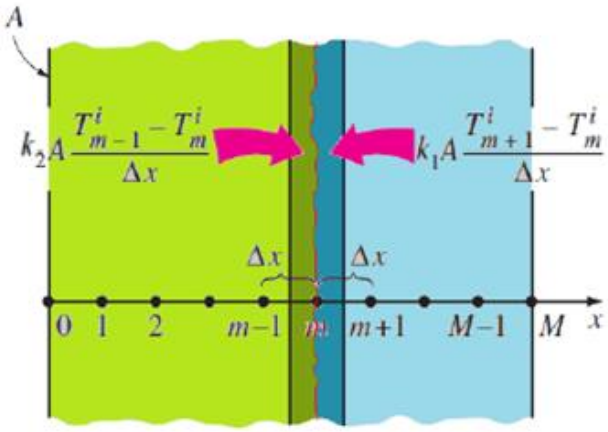

Source: Çengel, adapted.

We then have the conduction between two different materials k1 and k2:

$$k_1 \frac{T_{m-1} - T_m}{\Delta x} + k_2 \frac{T_{m+1} - T_m}{\Delta x} = \rho_1 \frac{\Delta x}{2} C_{p1} \frac{T_m^{i+1} - T_m^i}{\Delta t} + \rho_2 \frac{\Delta x}{2} C_{p2} \frac{T_m^{i+1} - T_m^i}{\Delta t} \quad (14)$$

Reorganizing:

$$k_1 \frac{T_{m-1} - T_m}{\Delta x} + k_2 \frac{T_{m+1} - T_m}{\Delta x} = (\rho_1 \frac{\Delta x}{2} C_{p1} + \rho_2 \frac{\Delta x}{2} C_{p2}) \frac{T_m^{i+1} - T_m^i}{\Delta t} \quad (15)$$

Isolating the term of interest, we have:

$$\boldsymbol{T_m^{i+1} = \left(k_1 \frac{T_{m-1} - T_m}{\Delta x} + k_2 \frac{T_{m+1} - T_m}{\Delta x}\right) \frac{\Delta t}{\left(\rho_1 \frac{\Delta x}{2} C_{p1} + \rho_2 \frac{\Delta x}{2} C_{p2}\right)} + T_m^i} \quad (16)$$

3.1.3 Discretization of the external face border

The discretized equation for node **(1)** of Figure 1, located at the contour of the outer wall, we assume the condition of natural convection of air, radiation given by the Stefan-Boltzmann law and solar radiation, we have that the net rate of energy that crosses the face of the infinitesimal element is given by equation (3.17), where G is the global radiation (solar radiation), is the absorptivity, is the emissivity, *Tsky* is considered as the ambient temperature and *To* is the surface temperature of the wall, according to (Çengel, 2012) and also observing in figure 4:

$$Q = \alpha G + \varepsilon\sigma(T_{céu}^4 - T_0^4) + h(T_{amb} - T_0) \qquad (17)$$

Figure 4

Node condition at the outer border

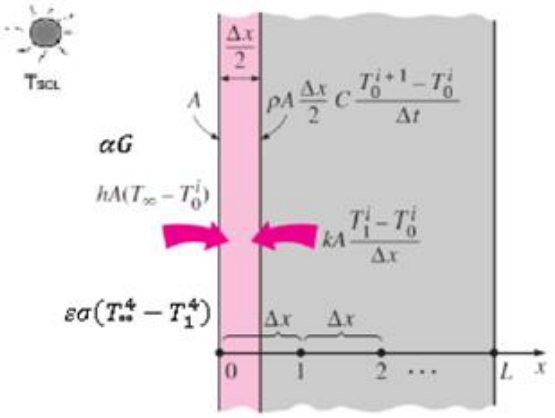

Source: Çengel, adapted.

Assuming the conduction condition coming from the posterior node next to equation (17), we have:

$$\alpha G + \varepsilon\sigma(T_\infty^4 - T_0^4) + h(T_\infty - T_0) + k\left(\frac{T_1 - T_0}{\Delta x}\right) = \rho\frac{\Delta x}{2}C_p\frac{T_0^{i+1} - T_0^i}{\Delta t} \qquad (18)$$

Isolating the term and rearranging the equation, we have:

$$T_1^{i+1} = \left(k\frac{(T_1 - T_0)}{\Delta x} + h(T_\infty - T_0) + \epsilon\sigma\left(T_\infty^4 - T_0^4\right) + \alpha G\right)\frac{2\Delta t}{\rho \Delta x C_p} + T_0^i \quad (19)$$

3.1.4 Discretization of the border of the inner face

Finally, we were able to obtain the discretized equation for the point (11) located at the boundary of the inner face of Figure 1. In Figure 5, we can see the contour node. In this case, we are considering that the heat transfer on the surface occurs only by pure natural convection.

Figure 5

Discretization at the inner boundary of the environment

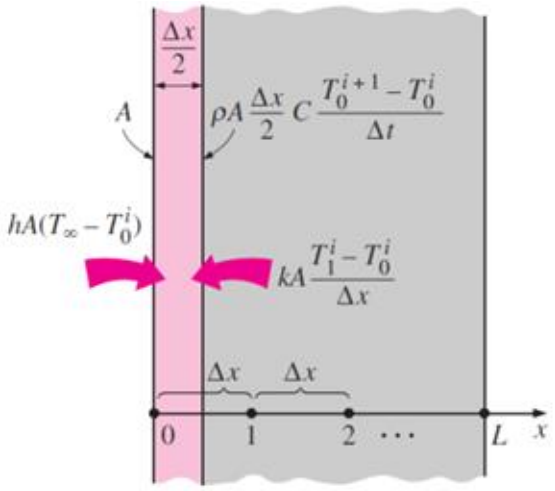

Source: Çengel & Afshin.

$$h_A\,(T_\infty - T_0^i) + k.A.\frac{T_1^i - T_0^i}{\Delta x} = \rho.A.\frac{\Delta x}{2}\,c_p\frac{T_0^{i+1} - T_0^i}{\Delta t} \quad (20)$$

Multiplying by

$$\cdot\left(\frac{2\Delta x}{k.A}\right) \rightarrow \frac{2h\Delta x}{k}(T_\infty - T_0^i) + 2.(T_1^i - T_0^i) = \frac{\rho.\Delta x^2}{k}\,c_p\frac{T_0^{i+1} - T_0^i}{\Delta t} \quad (21)$$

Towards:

$$: (\alpha = \frac{k}{\rho.c_p}) \rightarrow \frac{2h\Delta x}{k}(T_\infty - T_0^i) + 2.(T_1^i - T_0^i) = \frac{\Delta x^2}{\alpha \Delta t}(T_0^{i+1} - T_0^i) \quad (22)$$

Organizing:

$$: T_0^{i+1} - T_0^i = \tau\left[\frac{2h\Delta x}{k}(T_\infty - T_0^i) + 2.(T_1^i - T_0^i)\right] \quad (23)$$

Isolating the term of interest:

$$T_0^{i+1} = (T_0^i - 2.\tau.T_0^i - \tau.T_0^i \frac{2h\Delta x}{k}) + 2.\tau.T_1^i + 2.\tau.\frac{h\Delta x}{k}.T_\infty^i \quad (24)$$

Which in simplified form is:

$$\boldsymbol{T_0^{i+1} = (1 - 2.\tau - \tau.\frac{2h\Delta x}{k}).T_0^i + 2.\tau.T_1^i + 2.\tau.\frac{h\Delta x}{k}.T_\infty^i} \quad (25)$$

3.1.5 Stability Criterion

Implementing the explicit method is easier and faster, but it's unstable. To ensure stability, the appropriate criteria must be followed to avoid oscillations or divergences in the solutions. All equations were analyzed and an automatic procedure was used to choose the most restrictive criterion.

After defining the points and the spacing between them, it is necessary to calculate the time step following a specific relationship:

$$\Delta t \leq \frac{\Delta x^2}{2\alpha}, \quad onde \ \alpha = k/\rho.\mathrm{Cp} \quad (26)$$

It is good to note that this relationship depends on the thermal diffusivity of the material and the spacing of the mesh.

3.2 RESULTS OF THE SIMULATIONS

Several numerical simulations were performed (as shown in table 01) to evaluate the effects of the variation in the percentage of açaí residue and the effects of the different types of materials that can be applied for comparison purposes with gypsum board and açaí seed residue. The data on solar radiation and ambient temperature were obtained from INMET (National Institute of Meteorology). For these simulations, experimental data were used at the values of 0.21 W/m.K for the thermal conductivity of the gypsum board and açaí residue with a percentage of 20%, as well as a specific mass of 998 Kg/m³, specific heat of 1090 J/Kg.K, in addition to the absorptivity of 0.63 and emissivity of 0.93, data obtained by Çingel, (2012).

Table 1

Data from the numerical simulations of the ceilings

RESUMO DE DADOS PARA AS SIMULAÇÕES NUMÉRICAS DOS TETOS-PROJETO PIVIC-2021

PROJETO DE PESQUISA-NIZAR -PIVIC-UEMA-2021

			ESPESURAS-(m)					total	CONDUT. TÉRMICA-(W/m.K)				
SIMULAÇÃO	GRUPOS	DESCRIÇÃO DA PAREDE	e1	e2	e3	e4	e5	e	k1	k2	k3	k4	k5
S1		TETO PADRÃO-T1-ARG.0%BIOM.	0,025	0,025	0,03	0,025	0,025	0,13	0,53	0,53	0,30	0,53	0,53
S2	(G1)	TETO PADRÃO-T1-ARG.5%BIOM.	0,025	0,025	0,03	0,025	0,025	0,13	0,25	0,25	0,27	0,25	0,25
S3	Biomassa do	TETO PADRÃO-T1-ARG.10%BIOM.	0,025	0,025	0,03	0,025	0,025	0,13	0,18	0,18	0,25	0,18	0,18
S4	Açaí	TETO PADRÃO-T1-ARG.15%BIOM.	0,025	0,025	0,03	0,025	0,025	0,13	0,20	0,20	0,23	0,20	0,20
S5		TETO PADRÃO-T1-ARG.20%BIOM.	0,025	0,025	0,03	0,025	0,025	0,13	0,19	0,19	0,21	0,19	0,19
S6	(G2)	TETO EM LAJE CONVENCIONAL-T6	0,025	0,025	0,03	0,025	0,025	0,13	0,72	0,72	0,72	0,72	0,72
S7	(G3)	TETO PADRÃO-T7-MADEIRA	0,025	0,025	0,03	0,025	0,025	0,13	0,19	0,19	0,21	0,19	0,19
S8	Materiais de	TETO PADRÃO-T8-ALVENARIA	0,025	0,025	0,03	0,025	0,025	0,13	0,72	0,72	0,21	0,72	0,72
S9	Construção	TETO PADRÃO-T9-CONCRETO	0,025	0,025	0,03	0,025	0,025	0,13	1,40	1,40	0,21	1,40	1,40
S10		TETO PADRÃO-T10-GESSO	0,025	0,025	0,03	0,025	0,025	0,13	0,81	0,81	0,21	0,81	0,81

RESUMO DE DADOS PARA AS SIMULAÇÕES NUMÉRICAS DOS TETOS-PROJETO PIVIC-2021

PROJETO DE PESQUISA-NIZAR -PIVIC-UEMA-2021

	MASSA ESPECÍFICA-(Kg/m3)					CALOR ESPECÍFICO-(J/Kg.K)					ABSOR	EMISS
SIMULAÇÃO	p1	p2	p3	p4	p5	c1	c2	c3	c4	c5	alfa	epsilon
S1	1159	1159	1191	1159	1159	2168	2168	1090	2168	2168	0,68	0,93
S2	1031	1031	1142	1031	1031	2623	2623	1090	2623	2623	0,68	0,93
S3	943	943	1116	943	943	1817	1817	1090	1817	1817	0,68	0,93
S4	598	598	1093	598	598	3064	3064	1090	3064	3064	0,68	0,93
S5	458	458	998	458	458	3718	3718	1090	3718	3718	0,68	0,93
S6	1922	1922	1922	1922	1922	835	835	835	835	835	0,63	0,93
S7	545	545	998	545	545	2385	2385	1090	2385	2385	0,59	0,90
S8	1922	1922	998	1922	1922	835	835	1090	835	835	0,63	0,93
S9	2300	2300	998	2300	2300	880	880	1090	880	880	0,60	0,88
S10	800	800	998	800	800	1090	1090	1090	1090	1090	0,35	0,93

RESUMO DE DADOS PARA AS SIMULAÇÕES NUMÉRICAS DOS TETOS-PROJETO PIVIC-2021

PROJETO DE PESQUISA-NIZAR -PIVIC-UEMA-2021

	Temper. Máx-(oC)		Tempo Tmáx-(h)		Dif.Tempe.	Fator Decrem.	Dif.Tempo(Ret)	Referências	03/08/2022
SIMULAÇÃO	P.ext.	P.int.	T.ext.	T.int.	(oC)	RT*	(h)	Cengel	gráfico
S1	51,72	28,24	12,91	17,54	23,48	0,546	4,63	Lima(2005)/Ávila(2017),Exp.	OK
S2	53,94	25,30	12,64	19,55	28,64	0,469	6,91	Lima(2005)/Ávila(2017),Exp.	OK
S3	56,16	24,74	12,42	18,68	31,42	0,441	6,26	Lima(2005)/Ávila(2017),Exp.	OK
S4	55,73	24,95	12,47	18,69	30,78	0,448	6,22	Lima(2005)/Ávila(2017),Exp.	OK
S5	56,09	24,81	12,44	18,60	31,28	0,442	6,16	Lima(2005)/Ávila(2017),Exp.	OK
S6	49,56	31,36	12,85	15,66	18,20	0,633	2,81	Tab-A5;A8;A19,Exp.	OK
S7	53,48	24,83	12,44	17,60	28,65	0,464	5,16	Tab-A5;A8;Exp.	OK
S8	51,55	29,16	12,88	16,07	22,39	0,566	3,19	Tab-A5;A8;Exp.	OK
S9	49,20	30,06	13,22	16,17	19,14	0,611	2,95	Tab-A5;A8;Exp.	OK
S10	42,48	27,46	12,93	15,03	15,02	0,646	2,10	Tab-A5;A8;Exp.	OK

Source: Authors (2022).

3.2.1 Simple ceiling of ceramic tiles and concrete

In Figure 6, we can observe the external and internal temperature of the ceiling throughout the 24 hours of the day, highlighting the maximum temperature on the external wall, reaching 49.56 ºC, occurring around 12:85 pm and on the internal wall with a peak of 31.36ºC around 3:66 pm. Through the result, we can observe a delay in the temperature peak (RET= difference in the time when the maximum temperature occurs in the external ceiling in relation to the internal one), caused by the resistance and thermal conductivity of the material along the wall. Another analysis that can be obtained is the decrement factor (RT*= ratio between the maximum temperature of the inner ceiling and the maximum temperature of the outer ceiling).

The values obtained for the RT= 0.633 and RET=2.81h.

Figure 6

Temperature of the simple ceiling throughout the da

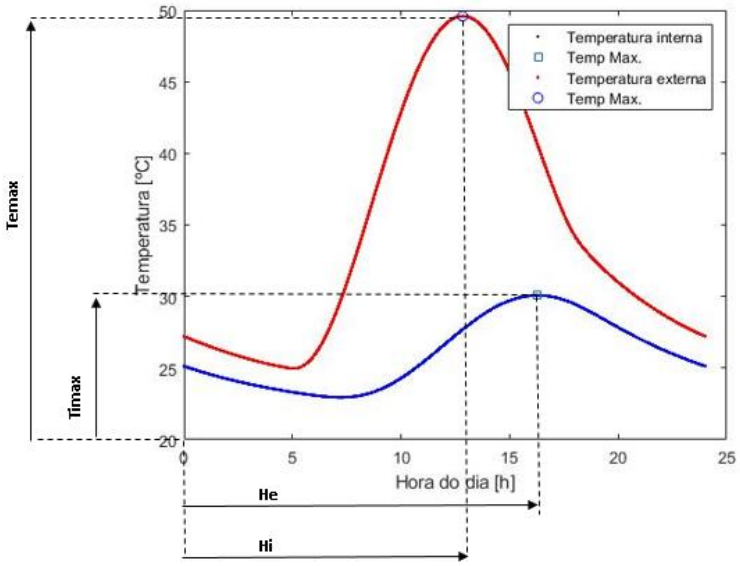

Source: Authors (2022).

3.2.2 Composite ceiling with different percentages of açaí residue

For the roof composed of açaí kernel residue, 5cm of ceramic tile was considered for each roof with the inner layer filled with 3cm plates with different percentage additions of açaí biomass, ranging from 0 to 20%, totaling a total thickness of 13cm.

From the simulations we were able to obtain Figure 7, which shows that the decrement factor is reduced as the percentage of residue added to the board increases, with the maximum reduction to 10% of additive waste. This leads us to conclude that the percentage

of efficiency of the composite ceiling with the addition of 10% of waste compared to the composite ceiling with gypsum board without the addition of it was **19.23%** in the reduction of the thermal load for the interior of the environment.

Figure 7

Effect of the variation in the percentage of açaí residue in the composite ceiling on the values of RT and RET*

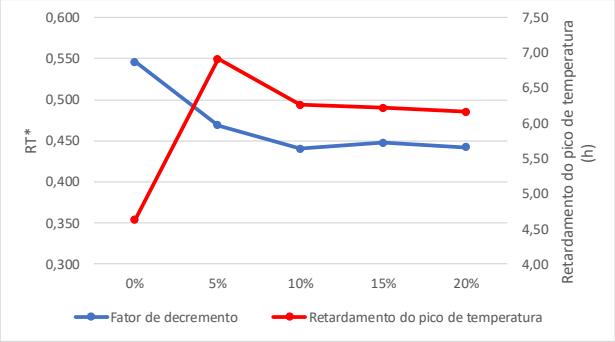

Table 2

Percentage of açaí residue applied to gypsum boards

AÇAÍ SEED RESIDUE ON GYPSUM BOARDS	RT*	RET
0%	**0,546**	**4,63**
5%	**0,469**	**6,91**
10%	**0,441**	**6,26**
15%	**0,448**	**6,22**
20%	**0,442**	**6,16**

Source: Authors (2022).

3.2.4 Ceiling with different materials used

For this simulation, four different types of materials were analyzed: The ceiling composed of standard ceramic tile slab simulated previously, the ceiling with external wooden faces with thermal conductivity of 0.19 W/m.K, specific mass of 545 Kg/m³ and specific heat of 2385 J/Kg.k and the ceramic masonry board and açaí residue with thermal conductivity of 0.21 W/m.K, specific mass of 1922 Kg/m³ and specific heat of 1090 J/Kg.k.

In Figure 8, we can see that the materials are organized in an increasing way in relation to thermal conductivity, from left to right, and with the increase in the thermal conductivity of the materials, the heat flow to the inner surface of the wall increases, decreasing the delay of the peak temperature (RET) and increasing the decrement factor (RT*).

When comparing wooden and concrete ceilings, we can see that the first is around **24.06%** more thermally comfortable.

Table 3

Variation in the type of ceiling construction material

CONSTRUCTION MATERIALS	RT*	RET
WOOD	**0,464**	**5,16**
MASONRY	**0,566**	**3,19**
CONCRETE	**0,611**	**2,95**
PLASTER	**0,646**	**2,10**

Figure 8

Effect of the variation of the type of ceiling material on the values of RT and RET*

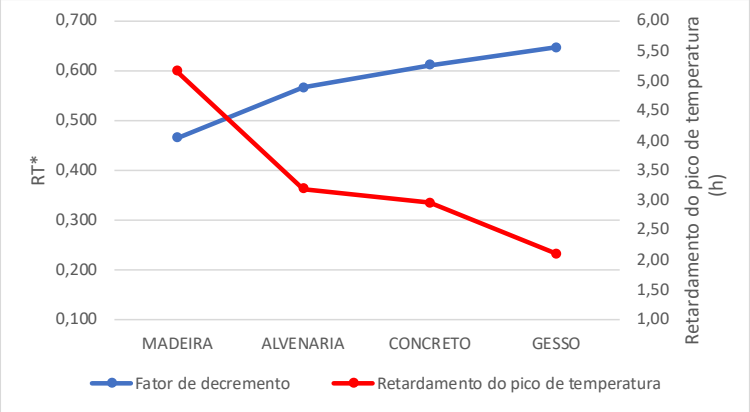

Source: Authors (2022).

4 CONCLUSION

It was verified that, the increase in the percentages of biomass addition, as well as the use of materials with low thermal conductivity characteristics in the composition of the flat roofs, it was observed the retardation of the heat flow along the composite slab, increasing the peak temperature delay, improving the thermal comfort of the internal environment, and consequently, reducing the use of air conditioners and fans.

- Comparing the proposed roof with the addition of 20% biomass (Table 01 = RT* = 0.442) and the conventional slab ceiling (Item 4.2.1 = RT*= 0.633), the thermal gain when replacing the conventional ceiling with the proposed one was **30.17%.** In view of the results presented, we can consider that the composite layer of gypsum and residue of the açaí seed

was essential in the thermal insulation of the composite roof, considering the differences found in the simulations.

REFERENCES

Barbosa, A. de M., Rebelo, V. S. M., Martorano, L. G., & Giacon, V. M. (2019). Caracterização de partículas de açaí visando seu potencial uso na construção civil. Revista Matéria, 24(3).

Çengel, Y. A., & Afshin, J. G. (2012). Transferência de calor e massa: Uma abordagem prática. Porto Alegre: Editora Mc Graw Hill.

Duffie, J. A., & Beckman, W. A. (2013). Solar energy thermal processes (4th ed.). New York, NY: Wiley Interscience.

FAQ – Imóveis e Construção. (2012, January 5). Retrieved from http://www.faq.inf.br/imoveis-construcao/parede-acustica-e-termica-o-que-e-vantagens-e-como-fazer/

Lima, J. P. (2005). Modelagem e teste de condutividade térmica em placa de gesso e fibra vegetal, Mauritia vinifera Martius, para uso na construção civil (Master's thesis). Faculdade de Engenharia Mecânica, Universidade Estadual de Campinas, Campinas, Brazil.

Nascimento, U. S. (2020). Borracha de pneus no isolamento térmico de paredes e tetos: Modelagem, validação e comparação com paredes convencionais (Doctoral dissertation). Universidade Estadual de Campinas, São Paulo, Brazil.

Patankar, S. V. (1980). Numerical heat transfer and fluid flow. New York, NY: Hemisphere Publishing Corporation.